CHEMISTRY
A EUROPEAN JOURNAL

Synthesis and Structural Metastability of CdTe Nanowires

Sandeep Kumar,[a] Martin Ade,[b] and Thomas Nann*[a]

Abstract: A new organometallic preparation method is described for CdTe nanowires with a high aspect ratio and a predominantly metastable wurtzite phase. The optical and morphological properties of the resulting nanowires were studied, as well as the influence of elevated temperatures on the crystallographic properties. A phase transition from wurtzite to sphalerite was observed at about 500 °C. The results show that the wurtzite phase is stabilized by the synthetic method and the surfactants.

Keywords: cadmium · colloids · nanowires · semiconductors · tellurium

Introduction

The II–VI semiconductor nanoparticles have attracted increasing interest among the research community because of their interesting size-dependent (or mesoscopic) properties. These important properties make these materials highly desirable for applications such as catalysis,[1] photovoltaics,[2–5] phosphors,[6] light-emitting diodes,[7–10] and biological tagging.[11–13] Mesoscopic properties arise mainly because of quantum-confinement effects or high surface-to-volume ratios. However, from the very beginning of nanoparticle research, the stabilization of crystallographic phases with different structures to the bulk counterpart was considered as another variable which might play a role in property modification in accord with the structure–property correlation.[14] It was recently observed that the shape of nanoparticles also plays an important role in the modification of the properties,[15] and thus properties of materials were tuned by way of their size, crystal structure, and shape.

The synthesis and applications of CdS and CdSe nanoparticles have been extensively reported, whereas synthetic reports of CdTe nanoparticles are very few.[16–24] Existing methods for synthesizing CdTe nanoparticles mainly involve approaches in aqueous media or the high-temperature organometallic route. Owing to the high monodispersity achieved by the organometallic approach, it seems most plausible for industrial applications, particularly for electronic devices based on conducting polymers where the polymers are very sensitive to moisture and air. Nanoparticles prepared by using the organometallic route can be solution-processed, and fabrication of various devices can be facilitated. The controlled synthesis of branched CdTe nanocrystals together with other morphologies have been achieved by using the organometallic route.[19–21]

Better understanding and control of the structural properties of these low-dimension nanoparticles are needed, as they may hold the key to many future applications. At present, the parameters that control the crystal structure and transition from one structure to another are not well understood. The phase diagram for nanoparticles may be different to that of the corresponding bulk material. Regards II–VI semiconductor nanoparticles, less attention has been paid to the effect of reduced size on the material structure than synthetic aspects. For the bulk material, it is well known that CdS and CdSe have highly stable wurtzite phases, whereas bulk CdTe has a sphalerite phase. Reports have been published in which crystal phases are stabilized other than the stable bulk phase for this class of nanocrystals.[19,25] Tang et al. demonstrated the shape and structural transformation of CdTe nanoparticles for the first time. The approach they adopted was based on an aqueous synthesis of spherical CdTe nanoparticles with a sphalerite-type crystal structure, in which by controlled removal of surfactants and oriented attachment of dots, nanowires with a wurtzite lattice were achieved.[26]

[a] S. Kumar, Priv.-Doz. Dr. T. Nann
Freiburg Materials Research Center
Albert Ludwig University Freiburg
Stefan Meier Strasse 21, 79104 Freiburg (Germany)
Fax: (+49) 761-203-4768
E-mail: thomas.nann@fmf.uni-freiburg.de

[b] M. Ade
Institute of Inorganic and Analytical Chemistry
Albert Ludwig University Freiburg
Albert Strasse 21, 79104 Freiburg (Germany)

Supporting information for this article is available on the WWW under http://www.chemeurj.org/ or from the author.

DOI: 10.1002/chem.200400585

The effect of pressure on the phase stability has been studied for CdSe nanoparticles by using a high-pressure diamond anvil cell; a structural transition from the four-coordinate wurtzite to the six-coordinate rock salt structure was observed on increasing the pressure.[27] Although temperature effects on the properties of nanoparticles have not been studied extensively, the temperature effects on the structure and shape of ZnS[28] and CdTe[29] nanoparticles have been reported; however, in both the cases the nanoparticles were of stable crystallographic phases (sphalerite type) and not many variations in the properties were observed except the grain growth on annealing at high temperatures.

Herein, we present the synthesis of CdTe nanowires with a predominantly wurtzite lattice, by using a high-temperature organometallic method. In addition, the effect of the reaction temperature on the shape and structure of the nanowires was investigated. These nanowires are promising candidates for polymer photovoltaic cells, especially as they can provide directionality to the current transport, and hence a better performance of the device is anticipated.[2]

Results and Discussion

Figure 1a shows the photoluminescence (PL) and absorption spectra of the CdTe nanoparticles. The particles have an emission in the near infrared (NIR) region with a full-width half-maximum (FWHM) of 75 nm. The absorption spectrum shows an absorption edge at about 740 nm. The exciton peak is not clear in the absorption spectrum, most probably because of the longer period of heating which might lead to Ostwald ripening. Figure 1b displays the TEM image of the synthesized nanowires. The nanowires had a mean length of 71.2 nm, while the diameter was approximately 7.0 nm. The particle size was estimated by measuring 100 particles in magnified TEM images and taking the average. In addition to the nanowires, some tetrapods were observed with arm dimensions comparable to that of the nanowires.

Figure 2 displays a HRTEM image of a CdTe nanowire. The spacing between adjacent lattice planes was observed to be 394 pm, which corresponds to the reflections due to the (110) plane of the wurtzite CdTe lattice, further confirming that the preferential growth direction is [0001].

Figure 3 depicts XRD patterns of the CdTe nanoparticles, synthesized and subsequently annealed at various temperatures for 1 h. Figure 3a presents the room-temperature XRD of CdTe nanoparticles. The diffraction pattern shows the presence of characteristic (100), (101), and (103) reflections of a wurtzite-type crystal of CdTe (space group $P6_3mc$; $a=$ 4.57, $c=7.49$ Å). A qualitative analysis of reflection broadening clearly shows influences of anisotropic crystallite size and the presence of stacking faults. A comparison of the narrow (002) with the broad (110) reflection indicates a needle shape of the crystallites with [0001] as the preferred growth axis. Broadening of diffraction peaks with $h-k\neq 3n$, that is (102) or (103), is characteristic for stacking faults disrupting the hexagonal arrangement of closed-packed layers

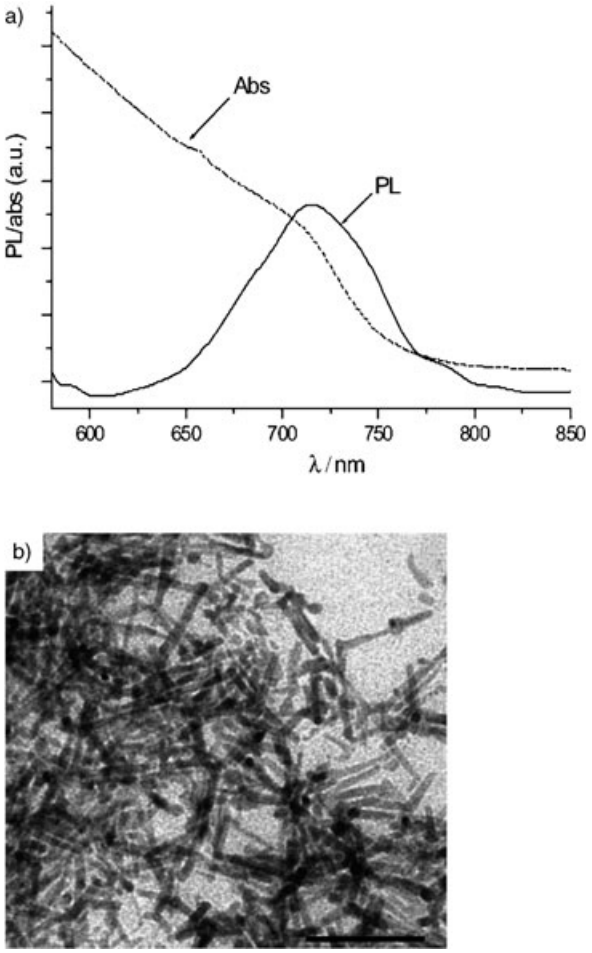

Figure 1. a) PL and absorption spectra of CdTe nanoparticles. b) TEM image of CdTe nanowires (scale bar = 100 nm).

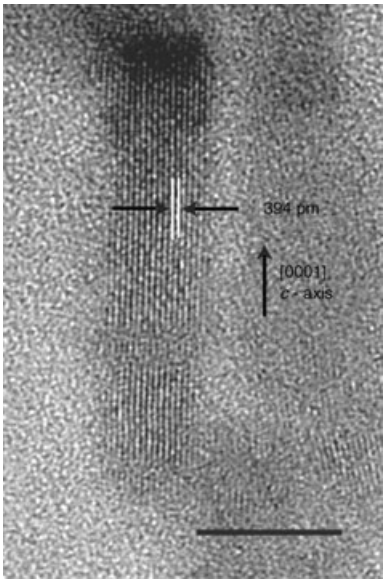

Figure 2. HRTEM image of CdTe nanowire (scale bar = 10 nm).

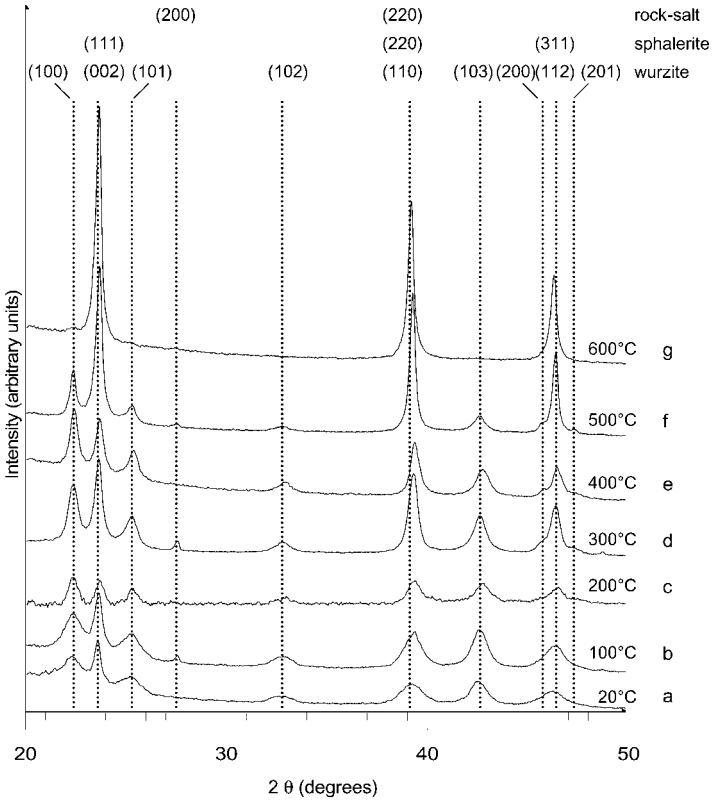

Figure 3. X-ray diffractogram of CdTe samples without annealing (a) annealed at 100 (b), 200 (c), 300 (d), 400 (e), 500 (f), and 600 °C (g). Theoretical reflection angles of CdTe wurzite, sphalerite, and rock-salt phases are denoted by dotted lines and Miller indices.

along [001] in wurtzite by cubic stacking sequences. Similar stacking faults have been already reported for dot-shaped CdTe nanoparticles[21] and CdSe nanoparticles[31] prepared by the organometallic route. Since the reflections of the cubic sphalerite-type crystal lattice (space group $F\bar{4}3m$; $a=$ 6.47 Å) strongly coincide with diffraction peaks of the wurtzite lattice planes, the phase composition of the pattern was refined by using the Rietveld method. It was found that the sample consists predominantly of nanoparticles of the hexagonal wurtzite modification at room temperature.

Figure 3b–g present results of the structural transformation study of nanoparticles by heat treatment, using XRD. It was observed that CdTe nanoparticles were still predominantly hexagonal after annealing at 100 and 200 °C. The refinement of the structure reveals that the cubic fraction is less than 3 %. On increasing the annealing temperature, the fraction of the cubic phase increased reaching 100 % at an annealing temperature of 600 °C. The nanoparticles gradually increase in size as the temperature is increased over this range. It is anticipated that the organic surfactants attached to the surface of the nanocrystals will degrade with increasing temperature.

In some of the diffraction patterns (at annealing temperatures of 100, 300, and 500 °C) a small amount of a phase with a cubic rock-salt structure is visible (space group $Fm\bar{3}m$, $a=6.46$ Å). CdTe with a rock-salt structure in bulk material has been reported to be stable only under pressures of 2 GPa.[32] It is not clear, if the rock-salt phase plays any role in the observed transformation from the wurtzite to sphalerite modification or is a by-product of the synthesis.

Thermogravimetric analysis (TGA) and differential thermal analysis (DTA) of an as-prepared sample were carried out simultaneously in an Netzsch STA 409 apparatus. Figure 4 displays TG and DTA measurements of the nanoparticles. The TG data indicates a weight loss of 62.9 % in the temperature range between 200 and 460 °C, which can be attributed to the degradation of organic surfactants from the surface of the nanocrystals. The DTA curve displays three endothermic peaks. The onset of the first peak at 45.5 °C can be interpreted as the melting of excess surfactant. The peak onset at 377.6 °C is attributed to the removal of organic ligands from the surface of the nanocrystals as most of the weight loss due to degradation of organic surfactants occurs in this region. The third peak has its onset at 483 °C, which defines the phase transformation temperature for the wurtzite-to-sphalerite modification.

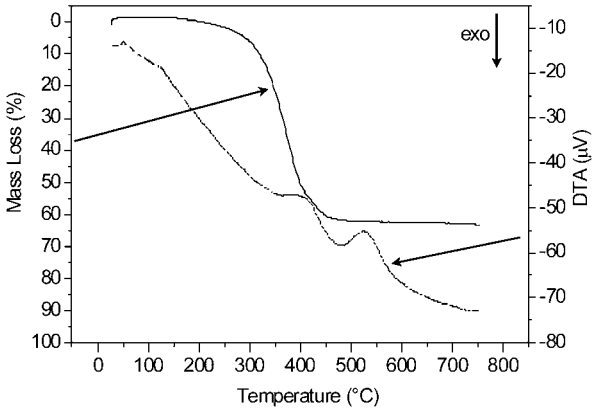

Figure 4. TGA and DTA data for CdTe nanowires.

Figure 5 presents the percentage cubic phase of CdTe nanowires as a function of the annealing temperature obtained by Rietveld refinement of the scaling parameters in the XRD pattern. The cubic fraction increased significantly in the temperature range between 400 and 600 °C reaching 100 % after annealing at 600 °C. This is in agreement with the DTA data, which suggests that the onset of the phase transformation occurs at 483 °C.

It is possible that during annealing at 500 °C the equilibrium may have established and heating for a longer period of time may have completely transformed the nanocrystals into the cubic modification. The phase transformation observed above can be explained by considering the metastability of the nonequilibrium wurtzite phase of CdTe nanoparticles. This is reasonable given the method of synthesis, which involves nucleation and rapid growth from a supersaturated solution. The stacking fault energy differences for the cubic

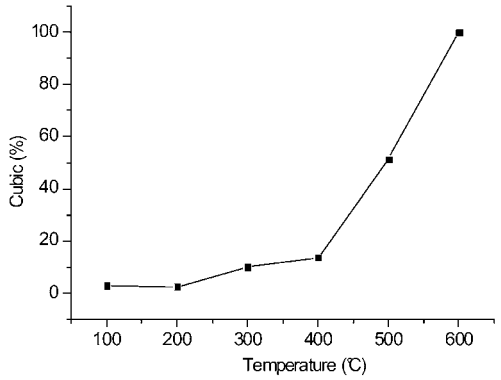

Figure 5. Percentage cubic phase fraction of CdTe nanowires as a function of annealing temperature.

and hexagonal phase has been found to be only 11 meV per atom for CdTe,[33] indicating that the free energy difference between the sphalerite and wurtzite crystal lattice is small, supporting the metastability of the crystal structure. During annealing, the thermal energy allows an activation of the metastable hexagonal structure to the lower-energy stable cubic phase, thus allowing the transition from the hexagonal to the cubic phase.

Figure 6a presents the electron diffraction pattern of CdTe nanocrystals annealed at 600 °C. The diffraction ring corresponds to the cubic phase of CdTe nanocrystals. Very sharp reflections due to the (111), (022), and (113) lattice planes can be seen. Figure 6b displays the TEM image of CdTe nanocrystals annealed at 600 °C, at which large clusters of CdTe are observed. The transformation of nanowires into large clusters can be explained by the degradation of organic ligands from the surface of the nanowires. These organic ligands act as stabilizers for nanowires, preventing them from agglomeration. Therefore it is possible that during the degradation of these surfactants from the surface, the nanoparticles agglomerate to form large clusters of CdTe due to high surface energy.

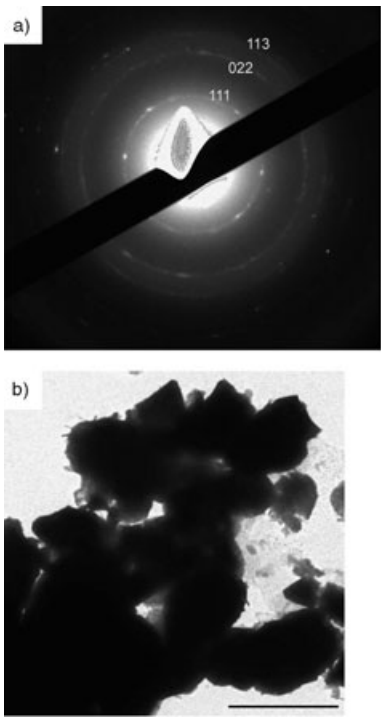

Figure 6. a) Electron diffraction pattern of CdTe nanowires after annealing at 600 °C. b) TEM image of CdTe nanoparticles annealed at 600 °C (scale bar = 1000 nm).

The lattice parameters of the unit cell were determined by the least-square fitting method. Table 1 presents the lattice parameters together with the unit cell volume of the nanoparticles after annealing at different temperatures. It was observed that the unit cell volume changes only slightly (0.5 %) on annealing. This indicates that the surface forces are not very dominant in these nanowires, and that the metastable phase was stabilized due to the synthetic method only.

Table 1.

Annealing temp. [°C]	Phase	Percent of phase	Lattice parameters [Å]	Specific volume
100	sphalerite	2.9	a = 6.268	270.6
	wurtzite	95.2	a = 4.566	135.32
			c = 7.493	
200	sphalerite	2.3	a = 6.451	268.4
	wurtzite	97	a = 4.565	135.16
			c = 7.488	
300	sphalerite	10	a = 6.468	270.6
	wurtzite	87.7	a = 4.570	135.92
			c = 7.516	
400	sphalerite	13.7	a = 6.459	269.49
	wurtzite	86.3	a = 4.569	134.99
			c = 7.465	
500	sphalerite	51.2	a = 6.468	270.62
	wurtzite	48.3	a = 4.574	135.73
			c = 7.492	
600	sphalerite	100	a = 6.4722	271.11

Conclusion

The above study provides a new scheme for the synthesis of CdTe nanowires with a predominantly wurtzite lattice by a high-temperature organometallic route. The effect of temperature on the shape and crystal structure of these nanoparticles was studied, leading to a better understanding of size-, shape-, and structure-dependent properties. It was observed that the metastable wurtzite lattice of nanocrystals achieved by this method is thermodynamically stable up to an annealing temperature of 200 °C, and on further increase of the temperature it gradually transforms into the more stable sphalerite modification forming large clusters of CdTe.

Experimental Section

CdTe nanoparticles were prepared by a slight modification of a previously published method.[19] Cadmium stearate (362 mg) was heated with tri-*n*-octylphosphineoxide (4 g; TOPO) under vacuum at 65 °C for 3 h. Te powder (56 mg) and tri-*n*-octylphosphine (2 mL; TOP) were added, and the temperature was raised slowly to 220 °C under Schlenk conditions. The particles were allowed to grow for 23 h, and then they were quenched by removing the heating mantle. At room temperature, anhydrous methanol was added to precipitate the particles. These particles were washed twice with MeOH and twice with *n*-butanol, and finally dried under high vacuum overnight.

The X-ray structure analysis was carried with a Siemens D5000 diffractometer operating at 40 kV and 40 mA, by using $Cu_{K\alpha 1}$ radiation. Samples were placed between two adhesive tapes and measured in transmission geometry with a position-sensitive detector (PSD). Rietveld calculations on powder diffraction data were carried out to obtain a quantitative estimation of phases using the GSAS computer program.[30] Pseudo-Voigt profile peak shape functions were used for the calculations. For annealing experiments the as-prepared CdTe nanoparticles were placed in an alumina crucible and heat-treated in a silica tube furnace at temperatures between 100 and 600 °C under flowing argon (0.1 MPa). A heating rate of 10 K min^{-1} and a holding time of 1 h at maximum temperature were chosen. The temperature was controlled by using an encapsulated Ni-Cr-Ni thermocouple with an accuracy of ± 5 K at the sample. The XRD characterization was done at ambient temperature and pressure with a 2θ range from 10° to 105°. Shape and further structural characterization were done by transmission electron microscopy (TEM) by using a LEO 912 operating at 120 kV. The photoluminescence (PL) and absorption spectra were recorded on a J & M TIDAS diode array spectrometer using dilute chloroformic solutions.

Acknowledgements

The authors thank Dr. Ralf Thomann and Prof. Michael Giersig for TEM measurements.

[1] T. S. Ahmadi, Z. L. Wang, T. C. Green, A. Henglein, M. A. Elsayed, *Science* **1996**, *272*, 1924–1926.
[2] W. U. Huynh, J. J. Dittmer, A. P. Alivisatos, *Science* **2002**, *295*, 2425–2427.
[3] W. U. Huynh, X. Peng, A. P. Alivisatos, *Adv. Mater.* **1999**, *11*, 923–927.
[4] S. Kumar, T. Nann, *J. Mater. Res.* **2004**, *19*, 1990–1994.
[5] D. S. Ginger, N. Greenham, X. Peng, A. P. Alivisatos, *Synth. Met.* **1997**, *84*, 545–546.
[6] J. Lee, V. C. Sundar, J. R. Heine, M. G. Bawendi, K. F. Jensen, *Adv. Mater.* **2000**, *12*, 1102–1105.
[7] N. Tessler, V. Medvedev, M. Kazes, S. Kann, U. Banin, *Science* **2002**, *295*, 1506–1508.
[8] B. O. Dabbousi, M. G. Bawendi, O. Onitsuka, M. F. Rubner, *Appl. Phys. Lett.* **1995**, *66*, 1316–1318.
[9] V. L. Colvin, M. C. Schlamp, A. P. Alivisatos, *Nature* **1994**, *370*, 354–357.
[10] I. Willner, F. Patolsky, J. Wasserman, *Angew. Chem.* **2001**, *113*, 1913–1916; *Angew. Chem. Int. Ed.* **2001**, *40*, 1861–1864.
[11] J. Bruchez, M. Moronne, P. Gin, S. Weiss, A. P. Alivisatos, *Science* **1998**, *281*, 2013–2015.
[12] J. Riegler, U. Kielmann, P. Nick, T. Nann, *J. Nanosci. Nanotechnol.* **2003**, *3*, 380–385.
[13] W. C. W. Chan, S. Nie, *Science* **1998**, *281*, 2016–2018.
[14] A. P. Alivisatos, *J. Phys. Chem. B* **1996**, *100*, 13227–13239.
[15] X. Peng, L. Manna, W. Yang, J. Wickham, E. Scher, A. Kavandich, A. P. Alivisatos, *Nature* **2000**, *404*, 59–61.
[16] A. L. Rogach, L. Katsikas, A. Kornowski, S. Dangsheng, A. Echymüller, H. Weller, *Ber. Bunsenges. Phys. Chem.* **1997**, *101*, 1668–1670.
[17] N. Gaponik, D. V. Talapin, A. L. Roagch, K. Hoppe, E. V. Schevchenko, A. Kornovski, A. Echymüller, H. Weller, *J. Phys. Chem. B* **2002**, *106*, 7177–7185.
[18] D. V. Talapin, S. Haubold, A. L. Rogach, A. Kornowski, M. Haase, H. Weller, *J. Phys. Chem. B.* **2001**, *105*, 2260–2263.
[19] S. Kumar, T. Nann, *Chem. Commun.* **2003**, *19*, 2478 –2479.
[20] L. Manna, D. J. Milliron, A. Meisel, E. C. Scher, A. P. Alivisatos, *Nat. Mater.* **2003**, *2*, 382–385.
[21] W. W. Yu, Y. A. Wang, X. Peng, *Chem. Mater.* **2003**, *15*, 4300–4308.
[22] S. Tan, Z. Tang, X. Liang, N. A. Kotov, *Nano Lett.* **2004**, *4*, 1637–1641.
[23] Y. Wang, Z. Tang, X. Liang, L. M. Liz-Marzan, N. A. Kotov, *Nano Lett.* **2004**, *4*, 225–231.
[24] M. Sima, I. Enculescu, C. Trautmann, R. Neumann, J. Optoelectron, *Adv. Mater.* **2004**, *16*, 121–125.
[25] A. B. Simmons, S. Li, V. T. John, G. L. Mcpherson, A. Bose, W. Zhou, J. He, *Nano Lett.* **2002**, *2*, 263–268.
[26] Z. Tang, N. A. Kotov, M. Giersig, *Science* **2002**, *297*, 237–240.
[27] S. H. Tolbert, A. P. Alivisatos, *J. Chem. Phys.* **1995**, *102*, 4642–4656.
[28] S. B. Qadri, E. F. Skelton, D. Hsu, A. D. Dinsore, J. Yang, H. F. Gray, B. R. Ratna, *Phys. Rev. B* **1999**, *60*, 9191–9193.
[29] R. J. Bandarnayake, G. W. Wen, J. Y. Lin, H. X. Jiang, C. M. Sorensen, *Appl. Phys. Lett.* **1995**, *67*, 831–833.
[30] A. C. Larson, R. B. Van Dreele, *GSAS - General Structure Analysis System. Los Alamos National Laboratory Report LAUR* 86–748.
[31] C. B. Murray, D. J. Norris, M. J. Bawendi, *J. Am. Chem. Soc.* **1993**, *115*, 8706–8715.
[32] D. Martínez-García, Y. Le Godec, M. Mézouar, G. Syfosse, J. P. Itié, J. M. Besson, *Phys. Status Solidi B* **1999**, *211*, 461.
[33] H. Gottschalk, G Patzer, H. Alexander, *Phys. Status Solidi A* **1978**, *45*, 207–217.

Received: June 9, 2004
Revised: November 11, 2004
Published online: February 18, 2005